Mech. Adv. Technol. Vol. 7, No. 2, 2023, pp. 193–199

DOI: 10.20535/2521-1943.2023.7.2.282705

UDK 620

Determination of the K_{IC} Fracture Toughness of the X210Cr12 High-Strength Material

Ergun ATEŞ[1]

Received: 22 June 2023 / Revised: 16 September 2023 / Accepted: 16 October 2023

Abstract. *Purpose: It is an important problem that the machines become unusable due to the deformation of the machine elements produced before the planned time. In this study, it was aimed to determine the KIC value of X210Cr12, which is a high strength material. In this way, more accurate load values can be used in the design.*

Methods: In the experimental study to determine the KIC value, the sample geometry, the crack depth, the load-dependent parameters and calculations and some conformity checks were carried out. Experimental system; KIC consists of 3-point flexure specimens, a press, an electronic circuit capable of detecting the change in load crack opening, and a logger.

Findings: In the study, the loads were determined from experimental graphs. Subsequently, load-crack opening values were determined. With these data, the KIC values were calculated as 719,7 and 839,7 MPa.mm1/2 as the minumum and maximum values, respectively.

Conclusion: The experimental graphs are in the form of curves that break abruptly with unstable crack propagation without showing plastic deformation. There is no study in the literature on the KIC value of X210Cr12 and it has been determined that it has a low KIC value compared to the high-strength steels studied. It is valuable to determine the KIC value, as fracture problems may occur in designs prepared with the material. The results of the study are data at room temperature.

Keywords: *fracture mechanics; fracture toughness; crack opening displacement; high strength steels; X210Cr12.*

Introduction

The loads affecting the machine elements are calculated by keeping them below the yield, tensile, and fracture strength values with traditional design methods. However, although many structures were designed and manufactured this way, it was observed that they suffered damage at operating stresses below the calculated stresses. The causes of these damages and the growth and spread of cracks caused by the loads acting on the materials have led to the determination of the principles of fracture mechanics that can fully express the resistance of the materials to fracture. In revealing and developing the basic principles of fracture mechanics, many researchers have done very valuable work. In the historical process, very important accidents in the name of humanity have supported the developments in this field.

Steels are one of the most preferred materials in most mechanical systems consisting of machine parts. This situation required much research to know the behavior of steel materials in the fracture event. One of them is: The effects of crack depth and sample width on fracture toughness and ductile-brittle transition were investigated by three-point bending experiments. The stress-strain change in front of the crack end was analyzed using the finite element method. The results showed that both normalized crack depth and sample width affect fracture toughness and ductile-brittle fracture event (Yan et al., 2000). A finite element study of the fracture behavior of sheet metals concluded that the magnitude of critical CTOD and/or critical load can be used as a fracture criterion for thin sheets (Kulkarni et al., 2002). For two structural materials, chromium steel and high-strength aluminum alloy, the results of shear fracture toughness with increased loading speed, with the resulting modes II stress density factors and fault start times determined. It has been explained that the general trend that a smaller amount of energy is required when the loading speed increases is not valid and reverses when the failure mode changes from cracks to adiabatic sliding

✉ *E. ATEŞ*
ergunates@gmail.com

[1] *Departament of Mechanical Engineering, Faculty of Engineering, Balıkesir University, Altıeylül, Balıkesir, Turkey*

ISSN 2521-1943 Mechanics and Advanced Technologies

bands (Kalthof et al., 2004). A recoverable plate impact test technology has been developed to examine the fracture mechanisms of Mode II crack. Steel C 60 is the test material. The results show that the nucleation and growth of several microcracks in front of the crack tip and the interactions between them cause unstable crack growth (Ma et al., 2008). A test loading device has been proposed to determine the fracture behavior of brittle materials under mixed mode I / II / III loading conditions. Three-dimensional finite element analysis and practical studies were conducted. The results showed that the proposed installation was able to determine the full range of fracture characteristics. It is concluded that there is a negligible discrepancy between the practical data and the estimated theoretical data (Zeinedini, 2019). Since the risk of brittle fracture increases as the thickness of the steel plate increases, it is important to properly stop the brittle cracks that occur to ensure safety. In the experimental study, the three-sided slit Charpy test and the DWTT test were applied, in which the direction of propagation of the crack was designed. It cannot be said that the assumed results of the absorption energy and the crack stop length have been achieved. Regarding the roughness of the fracture surface, the test piece is further roughened, in which the crack develops in the thickness of the direction of the plate (Aikawa, 2019). The cases of fatigue-induced damage to structures have been explained to be related to mechanical stress caused by mixed-mode loading conditions. To explain the damage, experiments were carried out with notched single edge materials made of 34CrNiMo6 using a tension-torsion tester in different mixed-mode ratios and phase angles. In particular, the effects on the bending and angle of bending, as well as on the residual lifetime, have been significant (Koester et al., 2019). An experimental and numerical analysis of the the failure mechanisms of S355JR steel was performed. Depending on the test temperature and sample geometry, a cleavage or ductile fracture was observed. The gap was formed by the nucleation-growth-merger process or the cutting mechanism (Neimitz et al., 2020). A modification was made to the normalization method and the method was applied to steels with small strain hardening and yield strength. Experiments were conducted to confirm modified normalization. The results showed that the modified method is sufficient for steels with a small strain hardening exponent and a high yield (Gao et al., 2021). 40Cr and 30CrMnSiNi2A are ultrahigh-strength steel (UHSS) used in engineering structures. Under dynamic loading, the fracture properties of such materials are very important for structural design. The mode II dynamic break properties of these two materials have been studied at high loading speeds. The results showed that in the loading speed range of this investigation, the fracture toughness of the two materials had a positive correlation with the loading speed (Fan et al., 2023).

Developments in fracture mechanics focus on many areas, such as dynamic fracture mechanics, interfacial fracture mechanics, slip fractures in earthquakes, stressed corrosion cracking, environmental effects on fatigue crack propagation, breakage of new materials such as nanocomposites and grade materials (Shukla, 2005). In this study, the fracture phenomenon in the material X210Cr12 was experimentally examined (Ateş, 1987) with K_{IC}, which is one of the fracture toughness measurement methods in fracture mechanics.

Materials and methods

It is a ledeburitic 12% chromium cold work tool steel with material number 1.2080 and DIN standard X210Cr12. It is resistant to corrosive and adhesive wear due to the presence of dense hard carbide inside. It has a high dimensional stability and very good compressive strength. The hardness of the material is 54–62 HRC. The lowest tensile strength value of the material at this hardness is 1920 MPa. Applications; Cutting, drilling, compression, and plastering dies. Plastic wood, paper industry, and broaching sets. Wire drawing rolls, pipe, and profile rollers can be counted as sandblast nozzles. The X210Cr12 material used in this study is a fragile material and requires a 3-point flexure test sample to measure the stiffness of the K_{IC} fracture toughness (BS-5762:1979; ASTM-E399-12:2013) Fig. 1.

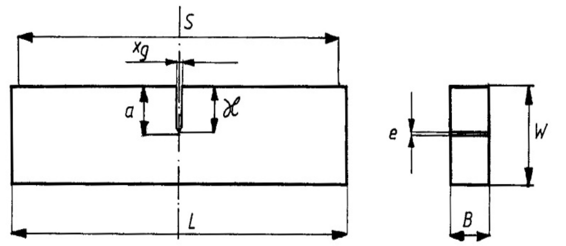

Fig. 1. K_{IC} 3 points flexural test piece dimensions. (a = 8 mm; e = 0.4 mm; χ=7.6 mm; L = 67.2 mm; S = 64 mm; W = 16 mm; B = 8 mm; Xg = 0.8 mm)

The K_{IC} 3-point flexural test piece was first prepared in 3D dimensions, then the notch form was prepared according to the dimensions given in Fig. 1. A separate set has been prepared for the tip of the 60° angle of the notch and the radius required to be 0.1 mm. With this radius set, the conditions in the standard are met. The process of creating a fatigue crack in the place where there is a notch is then opened in a fatigue device that vibrates at 300 rpm. When the fatigue crack in the test parts was met, the limitations of the crack length and the fatigue crack length were met. It was observed that the deviation of the crack from the spreading plane did not exceed 10°. The equipment used in the experimental study is as follows: Force gauge, Clip-Gauge tip opening meter, sample bending apparatus, *xy* printer and recorder, amplifier and test machine where the experiment is performed.

Force measurements: The material used in the experiment, X210Cr12, is a very hard and brittle material. For this reason, in order to prevent the force gauge prepared to bend this material from deforming at the time of compression, the material with a thickness of 4 mm on which the surfaces on which the strain gauge are attached has been prepared as shown in Fig. 2*a*. Fig. 2*b* shows the Wheat stone bridge circuit. For force measurement, a Wheatstone bridge circuit was installed on strain gauges with a resistance of 120 Ω and a gauge factor of 2.07. Resistors R_1 and R_3 active in the bridge circuit are the strain gauges on the force gauge. A 1 kΩ adjustable resistor has been added to the system to allow easy initialization adjustment. In the Wheatstone bridge circuit, the recording and supply output ends are seen.

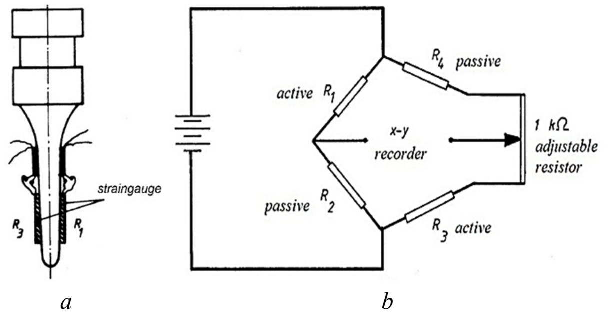

Fig. 2. Force gauge 4 mm and Wheatstone bridge circuit

The measurement of the opening of the tip of the notch was performed with the system given in Fig. 3*a*, *b*, and *c*. Fig. 3 shows: *a*) the special form prepared in the test piece, *b*) the Wheatstone bridge circuit, and *c*) the clip gauge. In measuring the crack opening, Fig. 3*a* shows the apparatus up to Z' from the sample surface, which is fixed with rigid adhesive. Fig. 3*b* shows the output ends for the circuit's feed and record and write functions in the Wheatstone bridge circuit. In Fig. 3*c*, there are 2 pieces of spring steel, which we call Clip-Gauge and where *T*1 and *T*2 are active Straingauge (straingauges are 120 Ω and Gauge factor 2.07) are determined by gluing: Its thickness is 0.5 mm, its width is 20 mm, and its length is 40 mm. The Clip-Gauge ends are fixed to the Z' particles given in Fig. 3*a*, and when there is a change in position, the signals are transmitted to the recorder via the bridge circuit.

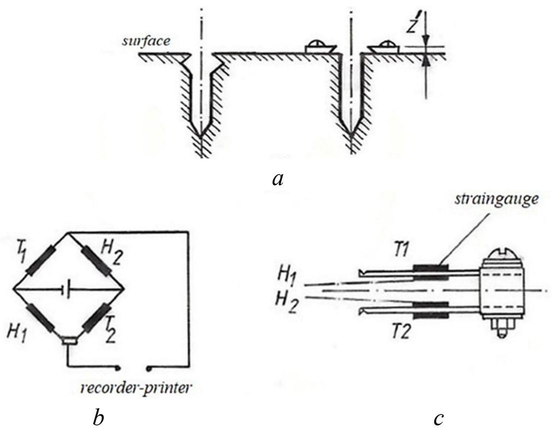

Fig. 3. Crack opening measurement system

The test piece sample bending apparatus is shown in Fig. 4. The dimensions of the apparatus that will allow the test samples to break on them are manufactured in accordance with the principles related to the test piece dimensions in the standards. Fig. 5 shows the test machine where the experiment will be carried out. The machine is a device that can pull a press with a load of 20 tons.

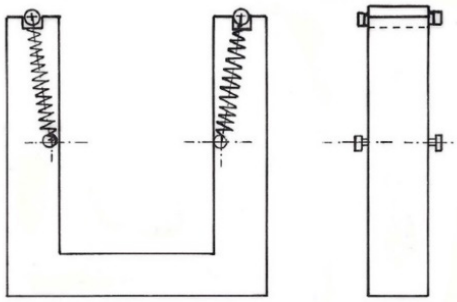

Fig. 4. Test piece bending system

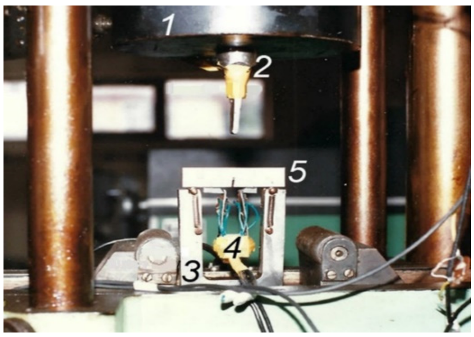

Fig. 5. Ready to measure the test stand. (*1* – press head; *2* – force gauge; *3* – test piece bending aparat; *4* – clip-gauge; *5* – test part)

Fig. 6 shows an *xy* printer. First, the signals from the strain gauges are amplified by a signal amplifier. The printer can then record these signals in relation to the amount of movement on the *x* and *y* axes.

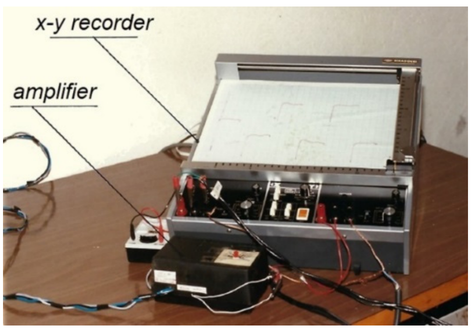

Fig. 6. *x-y* recorder and amplifier

According to the ASTM-E399-12:2013 standard: The value of the K_{IC} is calculated from this force using the equations created by elastic stress analysis of the sample the K_{IC} value determined by this test method depends on the formation of a sharp crack at the end of the fatigue crack in a sample of sufficient size. Therefore, in the calculation of the secant line OP_5, the point of rotation of the tilt adjustment should be at the point where the OA line intersects the displacement axis. The P_Q force is then defined as follows: If the force at each point in the record preceding P_5 is less than P_5 (Fig. 7, Type I), P_5 is P_Q; However, if before P_5 there is a maximum force exceeding it (Fig. 7, Types II and III), then the maximum force in this case is P_Q. Four three-point flexural test pieces were prepared from the test material X210Cr12 used in the experiment. In the tests carried out on the pull-compression test machine, a loading speed of 5×10^{-5} m/s was used. In the experimental study, the load opening (v) settings in the xy recorder were, respectively; (F) with settings of 20 mV/cm for the y-axis and 2 mV/cm for the (v) x-axis. The setting values are, respectively; the smallest two lines marked on the F-load axis show 96 N and the smallest two lines marked on the v-crack span axis show 0.057 mm.

The samples were broken at the time of the experiment, with the result that 4 curve graphs taken from the recorder are given in the form of F v (opening of the load crack) in Fig. 8. In the study of these curves: Since the test pieces used as in this study were a single material X210Cr12, the recorded curves were obtained with small differences, close values, and similar tendencies. The loading crack span F-v curves were recorded in this way. It was plotted on the correct curve corresponding to 2% crack growth on the selected inspection curve. The value at the point where the line cuts off the F-v curve, which has a slope about 5 % lower than the slope of the linear part of the curve, was determined as the critical force, that is, the growth of force at which the unstable crack begins.

In Fig. 7 given in the Standard, a situation similar to Type III [24] occurred in Fig. 8 and was taken as $F_Q = F_{max}$ in Fig. 8*d*. Similar operations were performed for the curves in Fig. 8 *a*, *b*, *c*, and the load values to be used in the calculation of fracture toughness were obtained over the curves.

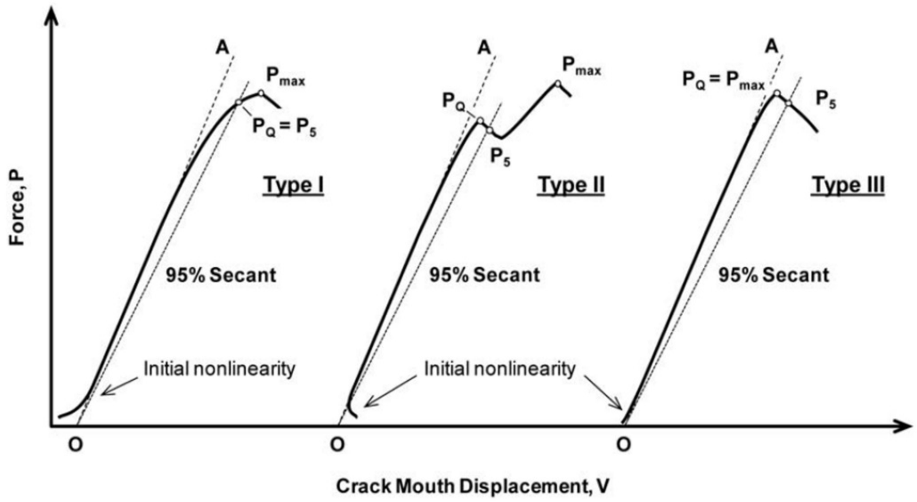

Fig. 7. Principal types of force-displacement records (ASTM-E399-12:2013)

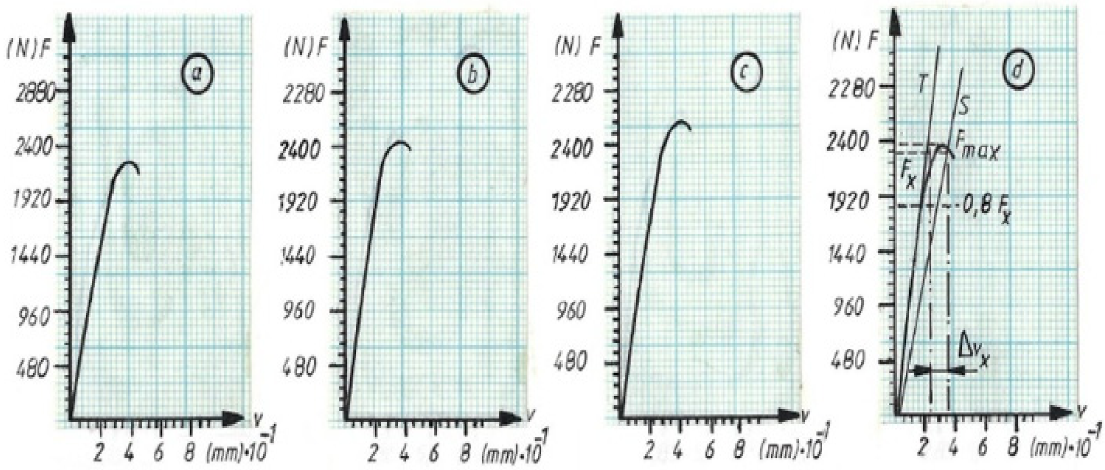

Fig. 8. Recordings of X210Cr12 material from x-y recorder as result of the experiment

Results and discussion

In the calculations, the experiment was considered valid because the ratio of the maximum force value to the critical force value was less than 1.1. The appropriateness of parameters such as fatigue precrack dimensions and geometry was checked and verified as parameters that generally affect the validity of the experiment. As a result of this verification, the K_{IC} values were calculated by replacing the critical load value with the appropriate formula for the test part used.

The parameters determined according to the operations performed on the graphs obtained from the X210Cr12 materials are given in Table 1. If checks are made according to the calculation flow required for the K_{IC} calculation according to the data in Table 1:

1. Since the type of curve is Mod-I, Type-III, $F_Q = F_{max}$. Accordingly, the F_{max} values in Table 1 were taken as F_Q in the calculations.

2. The equation was determined to be: $\Delta_v < (0.25)\,\Delta_{v_x}$

3. K_Q values (2) (ASTM-E399-12:2013) were calculated from the equation Y values (1) with the F_Q selected in item 1 and dependent on the test piece geometry, and the calculation results were given in Table 1.

For the (a/w) the ratio $\left(0<\left(\frac{a}{w}\right)<0.6\right)$ has been confirmed,

$$Y=(1.93)-(3.07)\left(\frac{a}{w}\right)+(14.13)\left(\frac{a}{w}\right)^2-$$
$$-(25.10)\left(\frac{a}{w}\right)^3+(25.80)\left(\frac{a}{w}\right)^4 \quad (1)$$

$$K_Q=\frac{F_Q\cdot(S/4)}{B\cdot\left(w^2/6\right)}\cdot\sqrt{a}\cdot Y \quad (2)$$

4. To verify the K_Q value with the expression that gives the correlation between the yield strength of the material, the crack length, and the thickness of the sample, it is necessary to know the yield strength of the material. Due to the high compressive strength properties of the X210Cr12 material, the hardness values are given as 200 HB and 260 HB respectively as small and large values in the literature. Due to the fact that the structure of the mate-rial is fragile and gives a load-crack opening curve in bending, like brittle materials, the large load value (for the test piece with a fatigue crack) is taken into account in the calculations. According to traditional methods of calculation of machine elements, a calculation can be performed taking 2/3 of the value of the greatest strength as the yield stress value for such brittle materials. With this approach, when the tensile strength and average hardness values were calculated, the yield strength value that could be used safely was taken as 500 MPa. This information is also given in the strength values information given by the steel manufacturer.

$$B\geq(2.5)\cdot\left(\frac{K}{\sigma_a}\right)^2. \quad (3)$$

The calculation was performed using the largest of the K_Q fracture toughness values in Table 1. In this way, equality (3) (ASTM-E399-12:2013) is also ensured for all other values.

Table 1. Parameters and calculation results determined from the curves of X210Cr12 test pieces

Sample	F_{max} (N)	F_x (N)	(0.8 F_x) (N)	Δ_v (mm)	Δ_{v_x} (mm)	K_{IC} (MPa.mm$^{1/2}$)
a	2259.452	2165.308	1732.247	0	0.114	719.700
b	2447.740	2306.524	1845.219	0	0.143	779.678
c	2636.028	2541.884	2033.507	0	0.157	839.655
d	2353.596	2290.833	1832.274	0	0.128	749.689

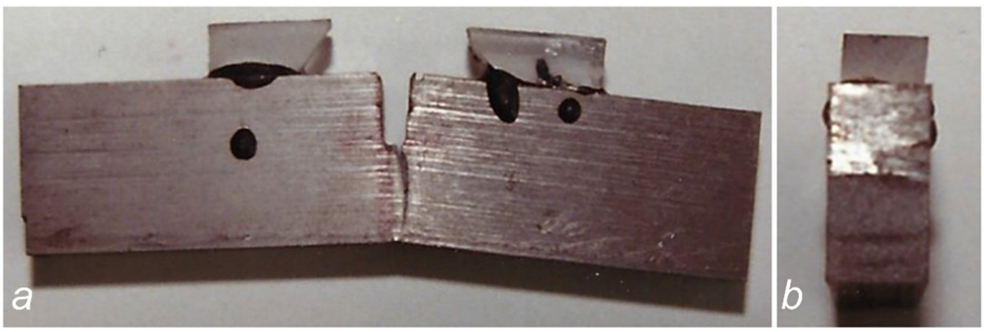

Fig. 9. The condition of the X210Cr12 material after the test (a) and the separation surface (b)

5. As a result of the operations performed in the above flow (from 1 to 4); The value of K_Q is taken as K_{IC} (since items 2 and 4 are provided). Table 1 shows the K_{IC} values of the test pieces.

Fig. 9 shows the condition (*a*) of a test piece and its shiny fractured surface (*b*) after the completed 3-point bending test. The condition of the broken surface gave the appearance of a deformed surface of a crunchy material.

Conclusion

The curves of the test pieces prepared from the material X210Cr12 are from the curves of the material, which suddenly break as a result of the spreading of an unstable crack, without showing plastic deformation. This result shows that the X210Cr12 material has a crispy structure. The test pieces were prepared from material X210Cr12; They broke in the range of 2259.452 to 2636.028 N. Since the fracture strength is calculated by the K_{IC} method for brittle materials: Test samples prepared from material X210Cr12; It has been determined to have a fracture strength of 719.700 to 839.655 MPa.mm$^{1/2}$. Attention should be paid to the X210Cr12 design, as the material can show a breakage problem with its large load value. The results obtained in this study were obtained at room temperature. Repetition of experiments with changes in temperature, a continuation of the work, can be a research.

In ASTM-E399-12:2013, the K_{IC} (MPa.mm$^{1/2}$) values of "martensitic precipitation hardened steels" and "4340 reclamation steels" are described as 1803.131 and 1535.286, respectively. Although there were no studies in the literature on the K_{IC} value of the study material X210Cr12, it was determined that it was obtained in a lower value range than those studied in the literature.

References

[1] T. Aikawa and T. Kawabata, "Consideration on the toughness difference depending on the direction of brittle crack prooagation in very thick steel," *Procedia Structural Integrity*, Vol. 21, pp. 173–184, 2019. DOI: 10.1016/j.prostr.2019.12.099

[2] ASTM-E399-12:2013. American Standart Institution. Standart Test Methods for Plane-Strain Fracture Thoughness of Metaşllic Materials. October.

[3] E. Ateş, Analysis of 3 Different Materials with Fracture Toughness Measurement Methods. Master Thesis. Uludag University. Graduate School of Natural and Applied Science. Bursa, Turkey. August, 1987.

[4] BS 5762:1979. British Standarts Institution. Methods for Crack Opening Displacement (COD) Testing.

[5] C. Fan *et al*., "Loading rate effect and failure mechanisms of ultra-high-strength steel under mode II fracture," *International Journal of Impact Engineering*, Vol. 171, 104374, pp. 1–13, 2023. DOI: 10.1016/j.ijimpeng.2022.104374

[6] H. Gao *et al*., "A modified normalization method for determining fracture toughness of steel," *Fatigue & Fracture of Engineering Materials & Structures*, Vol. 44, pp. 568–583, 2021. DOI: 10.1111/ffe.13380

[7] J.F. Kalthof and A. Bürgel, Influence of loading rate on shear fracture toughness for failure mode transition. Oral/Poster Reference: ICF10 1096 OR, Experimental Mechanics, Ruhr-University Bochum, Germany, 2004.

[8] P. Koester, C. Benz and M. Sander, "Investigation of mixed mode fatigue crack propagation in SEN-specimen under in-phase and out-of-phase conditions due to tension-compression and torsional loading," in *Proc. (ICMFF12) MATEC Web of Conferences 300*, 11006, 2019. DOI: 10.1051/matecconf/201930011006

[9] D.M. Kulkarni, R. Prakash and A.N. Kumar, "Experimental and finite element analysis of fracture criterion in general yielding fracture mechanics," *Sadhana*, Vol. 27, Part 6, pp. 631–642, Dec., 2002. DOI: 10.1007/BF02703355

[10] W. Ma and Z. Duan, "Investigation of mode II crack growth following a very high speed ımpact," *Journal of Mechanics of Materials and Structures*, Vol. 3, No. 2, pp. 271–290, Feb., 2008. DOI: 10.2140/jomms.2008.3.271

[11] A. Neimitz and J. Galkiewicz, "The experimental-numerical analyses of the failure mechanisms of S355JR steel," *Theoretical and Applied Fracture Mechanics*, Vol. 108, 102666, pp. 1–14, 2020. DOI: 10.1016/j.tafmec.2020.102666

[12] E. Orowan, "Fracture strength of solids," In Report on Progress in Physics, Physical Society of London: London, Vol. 12, pp. 185–232, 1949. DOI: 10.1088/0034-4885/12/1/309

[13] G.C. Sih, *Handbook of stress intensity factors*, Institute of fracture and solid mechanics: Lehigh University, Bethlehem, PA, 1976.

[14] A. Shukla, *Practical Fracture Mechanics in Design*. Second Edition, Revised and Expanded. Marcel Dekker, NY, 2005.

[15] V.T. Troshchenko, V.V. Pokrovskii, "Fatigue Fracture Toughness of Metals and Alloys. Part 1. Experimental Procedures and Materials and General Principles," *Strength of Materials*, 35, pp. 1–13, 2003. DOI: 10.1023/A:1022909018616

[16] A.A. Wells, 1973. The condition of fast fracture in aluminum alloys with particular reference to comet failures. British Welding Research Association Report, April 1955.

[17] C. Yan and Y.W. Mai, "Effect of crack depth and specimen width on fracture toughness of a carbon steel in the ductile-brittle transition region," *International Journal of Pressure Vessels and Piping*, Vol. 77, pp. 313–319, 2000. DOI: 10.1016/S0308-0161(00)00017-X

[18] A. Zeinedini, "A novel fixture for mixed mode I/II/III fracture testing of brittle materials," *Fatigue & Fracture of Engineering Materials & Structures*, Vol. 42, pp. 838–853, 2019. DOI: 10.1111/ffe.12955

Визначення в’язкості руйнування K_{IC} високоміцного матеріалу X210Cr12

Е. Атеш[1]

[1] *Університет Баликесір, Баликесір, Турція*

Анотація. *Мета: Важливою проблемою є те, що будівля стає непридатною для використання через передчасну деформацію виготовлених будівельних елементів. У цьому дослідженні метою було визначити значення K_{IC} для X210Cr12, який є високоміцним матеріалом. Таким чином, можна отримати правильні значення навантаження, які можна використовувати при проектуванні.*

Методика: В експериментальному дослідженні для визначення значення K_{IC} було проведено дослідження геометрії зразка, глибини тріщини, параметрів, що залежать від навантаження, а також розрахунки та деякі перевірки на відповідність. Експериментальна система; K_{IC} складається зі зразків для 3-точкового згину, преса, електронної схеми, здатної виявляти зміну розкриття тріщини під навантаженням, і реєстратора.

Результати: У дослідженні навантаження визначалися з експериментальних графіків. Згодом були визначені значення розкриття тріщин під навантаженням. На основі цих даних було розраховано значення K_{IC} 719,7 та 839,7 МПа.мм$^{1/2}$ як максимальне та мінімальне значення відповідно.

Висновок: Експериментальні графіки мають вигляд кривих, які різко обриваються з нестабільним поширенням тріщини, не показуючи пластичної деформації. В літературі відсутні дослідження величини K_{IC} для сталі X210Cr12 і визначено, що вона має низьке значення K_{IC} порівняно з досліджуваними високоміцними сталями. Визначення значення K_{IC} є важливим, оскільки в конструкціях, виготовлених з цього матеріалу, можуть виникати проблеми з руйнуванням. Результати дослідження є даними при кімнатній температурі.

Ключові слова: *механіка руйнування; в’язкість руйнування; зсув розкриття тріщини; високоміцні сталі; X210Cr12.*